CONCRETE LIBRARY OF JSCE NO.4, DECEMBER 1984

Equation for Shear Strength of Reinforced Concrete Deep Beams Based on FEM Analysis

(Proceedings of JCI 2nd Colloquium on Shear Analysis of RC Structures, Oct.25-26, 1983)

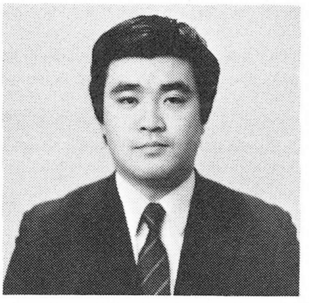

Junichiro NIWA

SYNOPSIS

Parameters which influence shear carrying capacity of deep and short beams have been clarified by numerical research using non-linear FEM analysis. Shear resistant mechanism of reinforced concrete members such as deep beams can be modeled by "tied arch mechanism". Effects of these parameters to the width and intensity of stress distribution of arch rib concrete have been estimated quantitatively. Finally equation for shear strength of deep and short beams without shear reinforcement has been derived.

J.NIWA is an assistant professor of civil engineering at Tokyo University, Tokyo, Japan. He received his Doctor of Engineering Degree in 1983 from Tokyo University. His research interests include strength, behavior and design of reinforced concrete members under shear and/or torsion, and fatigue strength of deformed bars. He is a member of JSCE and JCI.

---

1. INTRODUCTION

Based on FEM analysis using the computer program "COMM2" which has been developed at the concrete laboratory of Tokyo University[1], shear behavior of deep and short beams, such as shear span - effective depth ratio, that is, a/d is from 1.0 to 2.5, can be estimated after the occurrence of diagonal cracks and up to near the maximum shear carrying capacity.

It is the objective of this report to clarify shear resistant mechanism of members such as deep beams by utilizing the results of FEM analysis. FEM analysis will provide information concerning internal stress states of beams, which could not be known by experimental approach. Finally equation for shear strength of deep or short beams without shear reinforcement will be proposed by modeling shear resistant mechanism.

2. SUMMARY OF NUMERICAL STUDIES

2.1 Specimen Used for Numerical Studies

8 simple supported beams were analyzed by FEM. Four parameters which might influence shear behavior of deep or short beams were picked up, that is, shear span - effective depth ratio (a/d), longitudinal length of bearing plate - effective depth ratio (r/d), main reinforcement ratio (pw[%]) and concrete cylinder strength (fc'). Each parameter level was varied to two stages. Namely, a/d was 0.5 or 1.0, r/d was 0.2 or 0.4, pw was 2.0% or 5.0% and fc' was 19.6MPa or 49.0MPa. Each parameter was combined systematically. Effective depth of beams was, however, 300mm in all specimens.

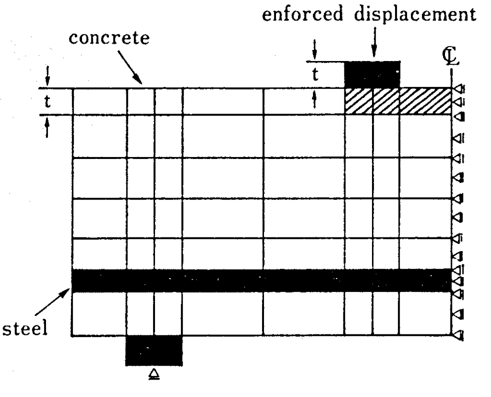

Fig. 1 configuration of divided mesh

2.2 Results of FEM Analysis

Elements configuration applied to each specimen is shown in Fig.1. External force was introduced at the load point as enforced displacement. Non-linear FEM analysis by Newton-Raphson method was carried out. Cracks were treated as "Smeared Crack".

Principal compressive stresses at about 90% of analytical maximum shear carrying capacity are shown in Fig.2. Until this stage, convergence of unbalanced forces of nodal points of elements is kept analytically. From Fig.2, it is recognized that principal

$a/d = 0.5$, $r/d = 0.2$, $pw = 2\%$, $fc' = 19.6$MPa

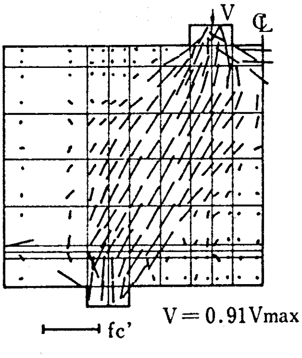

Fig. 2 principal compressive stress distribution

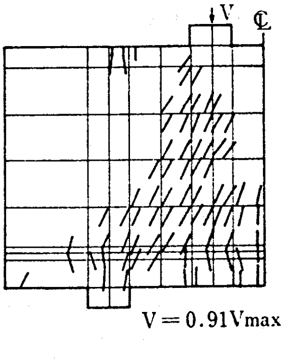

Fig. 3 crack propagation

compressive stresses flow from the load point to the support point directly. Principal compressive stresses also distributed widely in shear span and were extremely large just above the support point and also just below the load point.

Fig.3 shows the crack propagation at about 90% of analytical maximum shear carrying capacity. From Fig.3, some typical characteristics can be pointed out. The first is that cracks from near the load point to near the support point are remarkable, and the second is that cracks are initiated at the top surface of beam over the support point. FEM analysis can predict these phenomena which are very typical characteristics of deep beams and have been pointed out by many past experiments.

Finally it is predicted that each specimen will fail after crushing of web concrete nearby above the support point and/or below the load point. After this stage, the increase of enforced displacement caused the increase of unbalanced forces at nodal points of elements and it became analytical divergence condition. Judging from these results, it can be assumed that shear resistant mechanism is based on the tied arch model, whose arch rib is composed by compressive force of web concrete taking account of the flow of principal compressive stresses from the load point to the support point.

2.3 Influence of Each Parameter on Internal Stress Distribution

Utilizing the feature of this parametric study, influence of each parameter on the intensity and width of compressive stress distribution was investigated. Fig.4 shows influence of each parameter. In these figures, the effect of each parameter level was averaged by averaging the analytical results of four cases arithmetically. Shear force level in figures is about 95% of analytical maximum shear carrying capacity. Selected Gaussian points, where stresses are calculated, are just above the main reinforcement(Fig.5). The reason why these points were selected is that these points are near the failure portion of beams and stresses of these

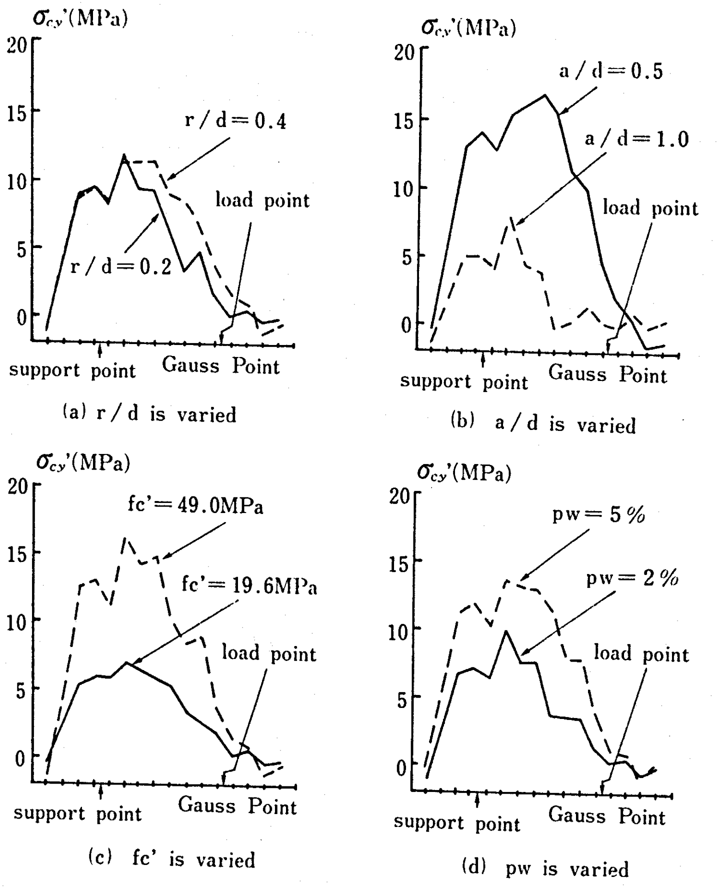

Fig. 4 variation of vertical compressive stress distribution above the support point points are almost similar in individual cases.

Ultimate shear strength should be influenced by this intensity and width of stress distribution. From these figures, following conclusion are derived. a/d doesn't influence the width but influence the intensity significantly. The effects of pw and fc' also appear on the intensity rather than the width. On the other hand, the effect of r/d is different from these effects. r/d doesn't influence the intensity seriously. The increase of r/d, however, causes the increase of the width of stress distribution.

Considering from this analytical result, it is valid that a/d, r/d, pw and fc' should be selected as parameters which influence the stress distribution of arch rib concrete in assuming tied arch shear resistant model.

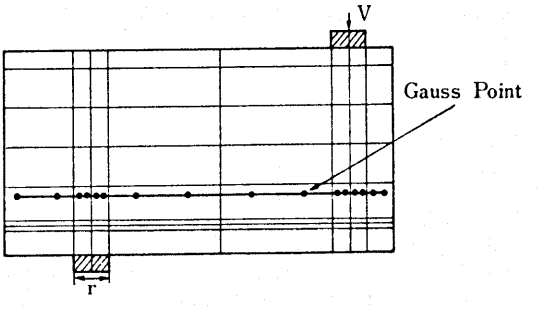

Fig. 5 position of Gauss Points for checking compressive stress distribution

3. SHEAR RESISTANT MODEL OF DEEP BEAMS

3.1 Simple Tied Arch Model and the Limit of Application

By assuming shear resistant mechanism to be a very simple model as shown in Fig.6, equilibrium conditions are written as follows.

$$D \sin\alpha - V = 0 \text{ ---- } (1),\quad D \cos\alpha - T = 0 \text{ ---- } (2),\quad T - C = 0 \text{ ---- } (3)$$

where, V : applied shear force, D : compressive force of arch rib concrete, T : tensile force of main reinforcing bar, C : compressive force of concrete in equal moment area, α: angle between the direction of arch rib concrete and the direction of main reinforcement, and

$$\sin\alpha = \frac{d}{\sqrt{a^2 + b^2}}$$

$$\tan\alpha = \frac{d}{a}$$

Assuming that the width of arch rib to be equal to the projection of longitudinal length of bearing plate to arch rib direction and concrete compressive stresses of arch rib to be uniform and be equal to $\sigma c'$, compressive force of arch rib is calculated as follows.

$$D = \sigma c' \, bw \, r \sin\alpha \text{ -------- } (4)$$

where, bw is breadth of web concrete. Then, shear force is also calculated as follows.

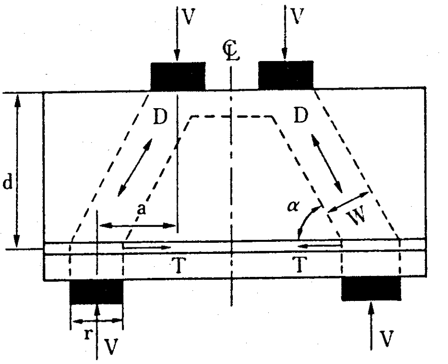

D : compressive force of arch rib concrete
T : tensile force of main reinforcement
W : width of arch rib concrete

Fig. 6 shear resistant mechanism based on simple tied arch model

$$V = D \sin\alpha = \sigma c' \, bw \, r \sin^2\alpha = \frac{\sigma c' \, bw \, r}{1 + (a/d)^2} \quad ---- (5)$$

When stress of main reinforcement which acts as tie bar is equal to σs, shear force is calculated from eq.(1) and eq.(2) as follows.

$$V = T \tan\alpha = As \ \sigma s \tan\alpha = As \ \sigma s \ (d/a) \quad ----- (6)$$

where, As is cross sectional area of main reinforcement.

Generally, failure of deep or short beams will be dominated by crushing of arch rib concrete or yielding of tie bar. Therefore, shear strength will be estimated by eq.(5) or eq.(6). If failure is dominated by yielding of main bar, maximum shear force will be calculated by eq.(6) substituting yield stress fy for σs.

Fig.7 shows experimental shear strength in comparison with predicted arch rib failure strength which is calculated by eq.(5) substituting concrete cylinder strength fc' for $\sigma c'$. Fig.7 shows that accuracy of prediction by eq.(5) is insufficient. Particularly the influence of fc', pw and r/d on shear strength is not represented perfectly. The reason why this accuracy of prediction is incomplete is that following assumptions were used in eq.(5). In eq.(5), the width of arch rib concrete was set equal to the projection of longitudinal length of bearing plate to arch rib direction, the effect of concrete strength was proportional to fc' and the effect of main reinforcement ratio pw which represents the stiffness of main reinforcement which should restrain and strengthen arch rib concrete was not incorporated into eq.(5).

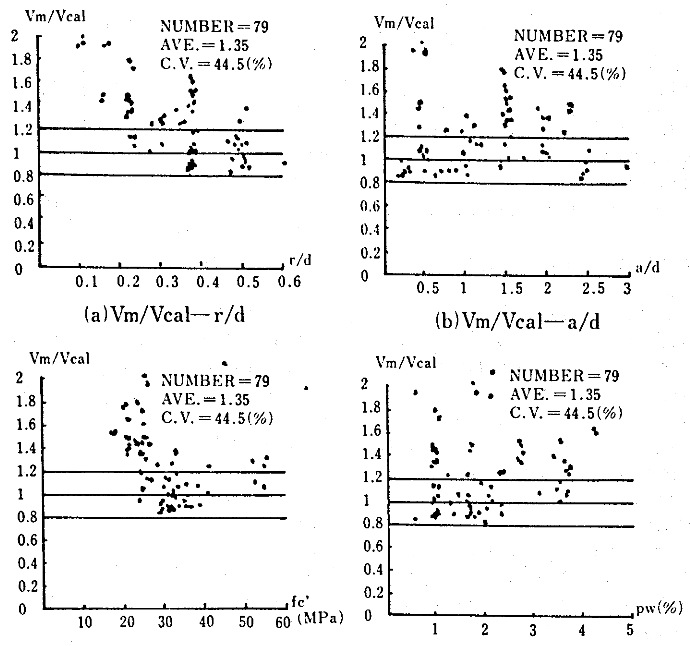

Fig. 7 ratio of experimental shear strength Vm to calculated shear strength Vcal by eq. (5)

In just before the stage where beams fail in shear, following facts, however, are found by results of FEM analysis in Chapter 2. The width of distributed compressive stresses is influenced by r/d and the increase of r/d causes the increase of width of distributed stresses. The intensity of compressive stresses in arch rib concrete is also influenced by changes of fc', pw and a/d. In order to establish accurate equation for predicting shear strength, therefore, it is necessary to estimate influences of each parameter on shear resistant mechanism quantitatively.

3.2 Influence of r/d on Shear Resistant Mechanism

In order to estimate the width of distributed compressive stresses in arch rib concrete quantitatively, judging from analytical results of Chapter 2, it is suitable that the effect of r/d will be considered. By reason of this, width of distributed compressive stresses was investigated by FEM analysis where only parameter r/d was changed.

Fig.8 shows distribution of vertical compressive stresses $\sigma cy'$ of beams in which only r/d is changed at the stage of about 90% of analytical maximum shear carrying capacity. In this case too, selected Gaussian points are just above the main reinforcement. From Fig.8, following two observations can be derived. The first is that vertical compressive stresses spread widely above the support point and the second is that in the central portion of stress distribution vertical stress level is very similar and is from about 40% to 50% of fc'. The width of distributed stresses is increasing accompanied with the increase of longitudinal length of bearing plate. The extent of increasing of width of distributed stresses is, however, relatively small compared with the extent of increasing of length of bearing plate.
Considering of this tendency, it is assumed that the width can be represented as follows.

$$x = r + k d = k d \left(1 + \frac{r}{k d} \right) \quad \text{-- (7)}$$

where, x is horizontal width of distributed stresses and k is a constant that represents the influence of length of bearing plate.

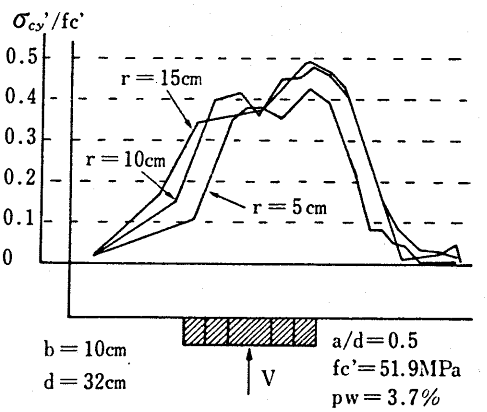

Fig. 8 the increase of width of compressive stress distribution according to the variation of r/d

Measuring x value on Fig.8 and calculating k at the places where vertical stress level $\sigma cy'$ is equal to 0.3fc' and 0.2fc', k value becomes to about 0.3. Therefore, it can be assumed that x is almost equal to r + 0.3 d or is directly proportional to 1 + 0.33 r/d. Experimental research was also carried out so as to verify this assumption. In tests, beam specimens were entirely identical to analytical specimens and only parameter r/d was changed similarly in analysis. Fig.9 shows experimental results in comparison with analytical results. The tendency of increasing of experimental shear strength is almost similar to analytical prediction. In conclusion, it is considered that the assumption concerning the width of distributed stresses may be valid.

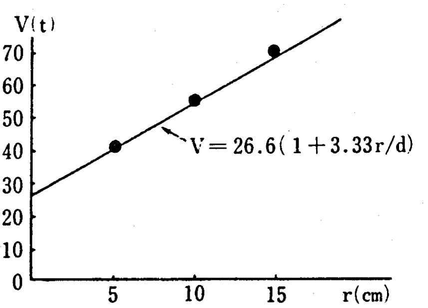

Fig. 9 the variation of shear strength according to the variation of r/d

3.3 Influence of a/d on Shear Resistant Mechanism

Next, in order to estimate the intensity of distributed compressive stresses in arch rib concrete quantitatively, it is necessary that the effect of a/d, pw and fc' will be considered, judging from analytical results of Chapter 2.

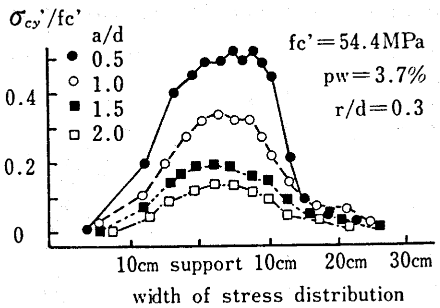

Fig. 10 the variation of vertical compressive stresses according to the variation of a/d

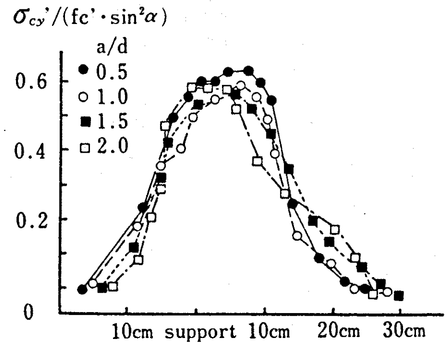

Fig. 11 $\sigma_{cy}'/(fc' \cdot \sin^2\alpha)$

In these parameters, it is considered that a/d represents the inclination angle of arch rib concrete. In this case too, the intensity of distributed compressive stresses was investigated by FEM analysis where only parameter a/d was changed from 0.5 to 2.0. Fig.10 shows distribution of vertical compressive stresses $\sigma cy'$ of beams in which only a/d is changed in the stage of about 90% of analytical maximum shear carrying capacity. From Fig.10, it is found that the intensity of vertical compressive stresses is decreasing accompanied with the increase of a/d.

However almost similar shape in individual cases of different a/d is gained, if these vertical compressive stresses are divided by $\sin^2\alpha$ (Fig.11). $\mathrm{Sin}^2\alpha$ is also suitable for the measure of intensity of vertical compressive stresses nearby above the support point.

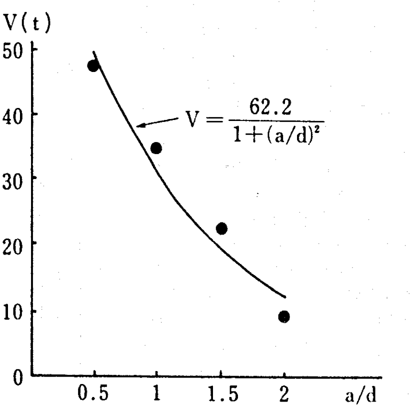

Fig. 12 the variation of shear strength according to the variation of a/d

Experimental research were carried out so as to estimate the effect of a/d. In tests, beam specimens were entirely identical to analytical specimens and only parameter a/d was changed. Fig.12 shows experimental results in comparison with analytical results. The tendency of decreasing of shear strength is almost similar to analytical results. In conclusion, it is considered that this assumption of a/d concerning the intensity of distributed stresses may be valid.

3.4 Influence of fc' and pw on Shear Resistant Mechanism

Lastly, in order to estimate the intensity of distributed compressive stresses in arch rib concrete quantitatively, it is necessary that the effect of fc' and pw will be considered, judging from analytical results of Chapter 2. Therefore, the intensity of distributed compressive stresses was investigated by FEM analysis where only parameter fc' or only parameter pw was changed. Fig.13 and Fig.14 show the distribution of vertical compressive stresses $\sigma cy'$ of beams in the stage of about 90% of analytical maximum shear carrying capacity. In Fig.13 and Fig.14, only fc' and only pw is changed respectively.

It is found that the effect of fc' is relatively small than the extent of being proportional to the increase of fc'. The reason why the effect of fc' is not proportional to the extent of fc' is that compressive stress distribution is not perfectly uniform and concentrates on some parts. Fig.15 shows the shapes in individual cases of different fc' in which vertical compressive stresses are divided by $fc'^{2/3}$. Judging from this figure, it is considered that the effect of concrete strength can be estimated by $fc'^{2/3}$.

It is predicted that pw represents the stiffness of main reinforcement as tie bar which should restrain arch rib concrete. Fig.14 shows the effect of pw clearly. It might be considered that there is the upper bound value in the effect of pw. However, it is recognized that the effect of pw may be proportional to the value $1 + \sqrt{pw}$, where pw has the unit of percent, from analytical results. Fig.16 shows the shapes of Fig.14's vertical compressive stresses divided by $1 + \sqrt{pw}$. In Fig.16, divided shapes of stress distribution are almost similar.

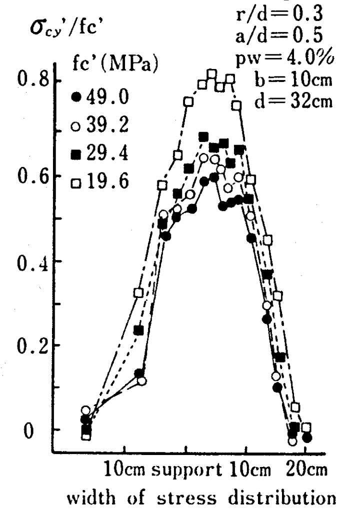

Fig. 13 the variation of σ_{cy}' according to the variation of fc'

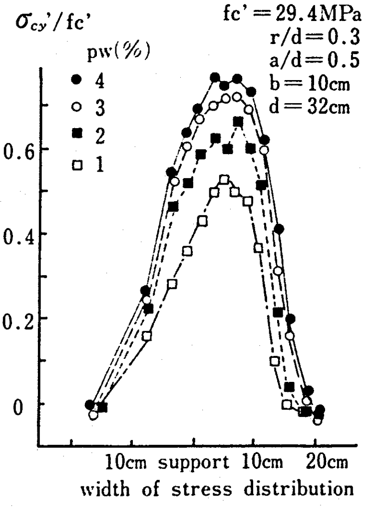

Fig. 14 the variation of σ_{cy}' according to the variation of pw

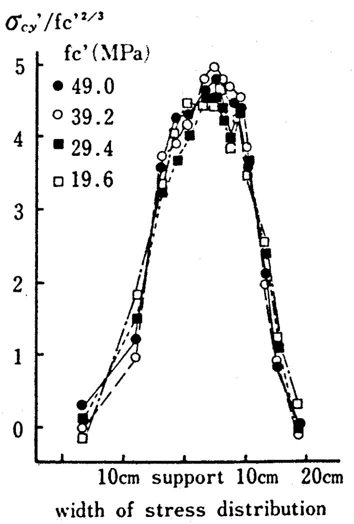

Fig. 15 $\sigma_{cy}' / fc'^{2/3}$

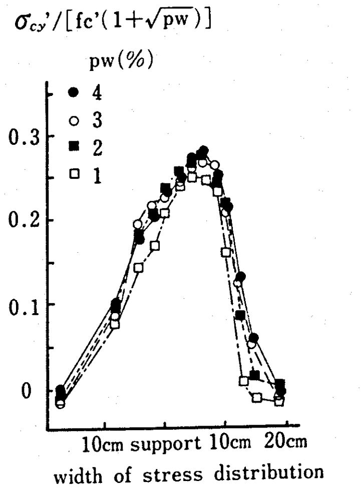

Fig. 16 $\sigma_{cy}' / [fc'(1+\sqrt{pw})]$

Finally, based on analytical investigations mentioned above, eq.(5) can be rewritten in the following form.

$$V = \frac{K\, fc'^{2/3}\, bw\, d\, (1 + 3.33\, r/d)(1 + \sqrt{pw})}{1 + (a/d)^2} \quad \text{----} \quad (8)$$

where K is a constant.

In order to verify the accuracy of eq.(8), some typical experimental data were picked up. These data were reported by past researchers and parameters of these data were widely distributed. Fig.17 shows experimental shear strength in comparison with calculated shear strength predicted by eq.(8). In calculation, K value is set equal to 0.53 for average of ratio of experimental strength to analytical strength to be equal to 1.0. From Fig.17, it is admitted that eq.(8) may be valid for prediction of shear strength of deep or short beams.

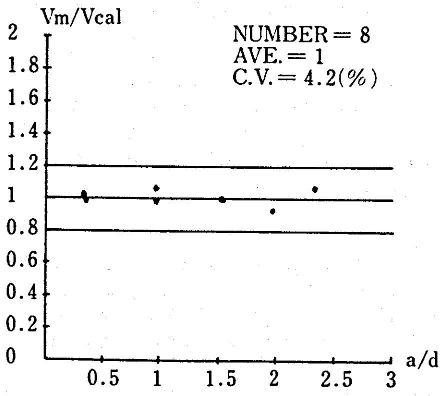

Fig. 17 evaluation of eq. (8) by selected data

4. EQUATION FOR SHEAR FAILURE LOAD OF DEEP BEAMS

4.1 Estimation Based on Experimental Data

Eq.(8) can be derived from the investigations in Chapter 3. Eq.(8) may predict shear strength of typical data of deep or short beams. Next, possibility of application of eq.(8) for general data published until now must be investigated. For this objective, 132 data have been collected. Fig.18 shows experimental shear strength of these data in comparison with calculated shear strength predicted by eq.(8). Contrary to expectation, accuracy of prediction of eq.(8) is not sufficient.

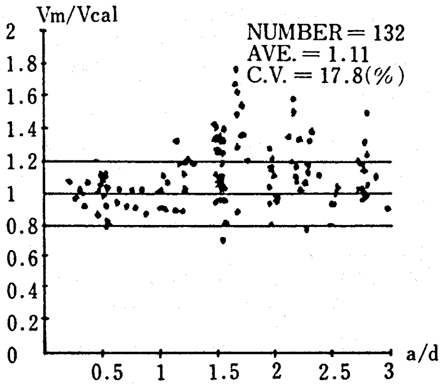

Fig. 18 evaluation of eq. (8) by all data

The average of ratio of experimental value to calculated value is considerably different in individual researchers (Table 1). For example, experimental data of some researchers are relatively high and on the other hand are low. Therefore it is predicted that experimental conditions might be very important.

After precise verification of these published experimental data, "knife-edge supports" or "rocker supports" were used when experimental shear strength were relatively high than predicted shear strength. In these supports, friction between a roller and steel plates can not be neglected and the restrain for rolling and horizontal displacement should cause. In consequence of this restrain, axial compressive force may be introduced to beams and shear strength may be increased.

On the opposite, right angle hooks were set up at the ends of round main reinforcing bars when experimental shear strength was relatively low than predicted shear strength. Right angle hooks can not ensure the anchorage of round bars generally. It is considered that in this case tensile force of main reinforcement could not be developed to full strength and finally anchorage failure occurred and in consequence of this, shear strength may be decreased considerably.

In FEM analysis, following assumptions are used. That is, rolling and horizontal displacement at supports are perfectly free and anchorage of main reinforcement is ensured entirely. Therefore, this increase or decrease of shear strength against expectation can not be estimated by FEM analysis and in consequence of this, eq.(8) also can not predict these experimental data.

4.2 Verification Tests for Past Published Data

In order to verify the accuracy of past published data, entirely same experiments as published data were carried out. These past published data had suspicion about support conditions or anchorage conditions.

Clarifying these suspicion, beams for verification tests have knife-edge supports or insufficient right angle hooks of the ends of round bars.

In order to investigate the effect of restrain on supports, a pair of entirely identical beams were tested. One was supported on the knife-edge supports (Fig.19). The other one was supported on normal roller supports which didn't restrain rolling and horizontal displacement. Fig.20 shows the load - deflection relationships. As shown in this figure, beams supported on knife-edges have relatively high stiffness and relatively high shear strength than beams supported on normal roller supports in any a/d conditions used in experiments. Considering of this result, support conditions should influence shear carrying capacity of deep or short beams significantly and axial compressive force caused by restrain of supports should produce the increase of shear strength. Concerning of support conditions, besides the longitudinal length of bearing plate, the existence of restrain on supports or not is very important.

The influence of restrain on supports can be also predicted by numerical study. Fig.21 shows the analytical result of beams used for verification tests. In FEM analysis, a beam restrained on supports has also relatively high stiffness and high shear carrying capacity than a beam supported on free conditions.

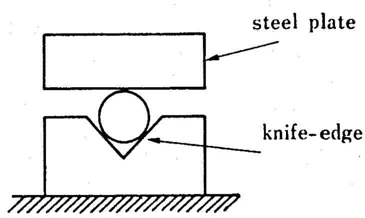

Fig.19 knife-edge support used in verification test

Table 1 ratio of experimental shear strength to calculated shear strength by eq. (8)

No.	researcher	number	a / d	r / d	fc'(MPa)	p w (%)	average
1	Leonhardt	5	1.0 ~3.0	0.481	302	2.07	0.95
2	Swamy	8	1.0 ~2.5	0.508	290~353	1.12~3.06	0.91
3	Moody	12	1.525	0.381	176~254	2.72~4.25	0.99
4	Mathey	19	1.51~2.84	0.221	223~311	0.84~3.05	1.27
5	Manuel	5	0.30~0.65	0.374	307~359	0.97	0.97
6	Paiva	2	1.0	0.502	203~238	1.67~2.58	1.01
7	Rueter	9	0.25~1.06	0.374	323~388	0.63~1.88	1.02
8	Kong	1	0.351	0.105	256	0.51	1.07
9	Clark	15	1.17~2.34	0.228	219~267	0.98	1.08
10	Krefeld	11	2.24~2.78	0.26~0.32	197~312	0.80~3.41	1.13
11	Higai	2	2.0	0.5	316~328	2.39	1.08
12	Shirakawa	2	2.0	0.1	452~656	2.12	0.96
13	Morrow	23	1.19~2.27	0.27~0.29	115~481	0.57~3.83	1.34
14	Smith	5	0.77~2.01	0.334	199~221	1.93	1.00
15	Maekawa	5	0.8	0.36~0.60	285~305	2.29	0.98
16	Author	8	0.50~2.00	0.06~0.31	529~555	3.72	0.95

total 132, average 1.11, c.v. 17.8%

Next, in order to investigate the effect of anchorage method, two pairs of entirely same four beams were tested except for kind of main bars. One pair of beams had only right angle hooks at the ends of round or deformed main reinforcement. The other pair of beams had stirrups for anchorage at the ends of round or deformed main reinforcement and further had welded cross bars at the ends of main bars for anchorage. Fig.22 shows the load - deflection relationships of these four beams. As shown in this figure, beams which had deformed bars as main reinforcement represented similar stiffness and similar shear carrying capacity in spite of different anchorage methods. On the other hand, in the case of beams which had round bars as main reinforcement, stiffness of a beam was changed between insufficient anchorage and complete anchorage and shear carrying capacity of a beam with insufficient anchorage was relatively low than a beam with complete anchorage.

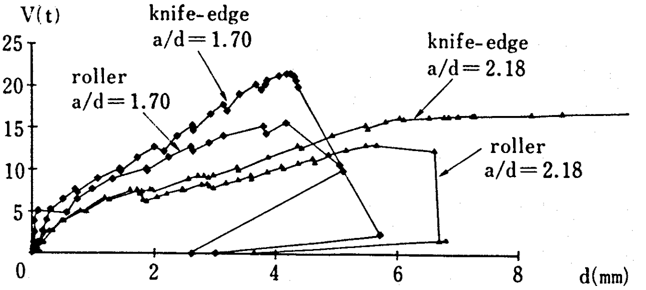

Fig.20 shear force - displacement relationship

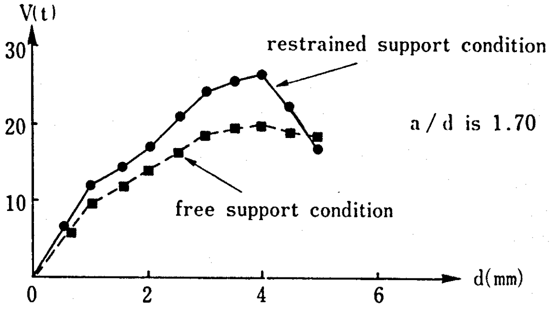

Fig. 21 shear force - displacement relationship predicted by FEM analysis

This phenomenon may be due to the occurrence of anchorage failure of round bars. In this case, by only the observation after test, it may be decided that failure mode is shear failure, judging from the crack propagation. However, in the fact, bending failure should be caused by immature anchorage failure. In consequence of this misunderstanding, this case may result relatively low misleading "shear strength".

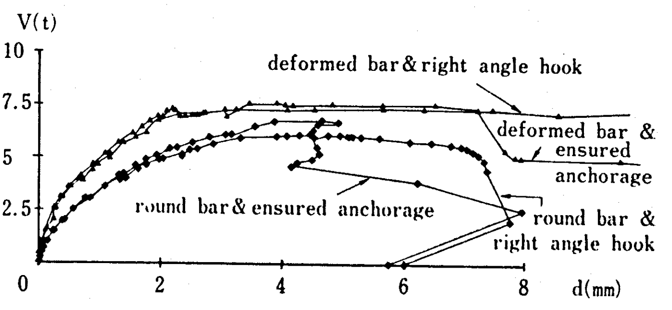

Fig.22 shear force - displacement relationship

4.3 Estimation of Accuracy in Prediction of Equation for Shear Strength

Based on the information obtained from verification tests, the refinement for past published data has been carried out under following conditions. The first condition is the existence of restrain on supports. In verification of eq.(8), experimental data were excluded, if beams were restrained on supports. The second condition is the use of round bars. The reason why data of round bars were excluded is that in this case, anchorage of main reinforcement may be insufficient.

For refined data obtained by this selection method mentioned above, Fig.23 shows experimental shear strength in comparison with calculated shear strength predicted by eq.(8). It is admitted that eq.(8) can predict experimental shear strength reasonably accurately. The average of ratio of experimental value to predicted value by eq.(8) is 1.00 and the coefficient of variation is 11.6% for 79 data.

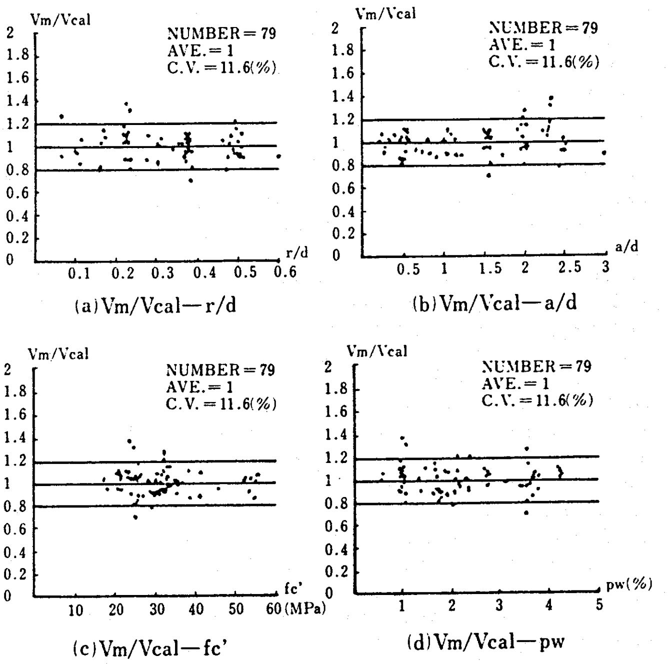

Fig.23 evaluation of eq. (8) by refined data

4.4 Relationship of Eq.(8) and the Equation for Shear Strength of Slender Beams

Eq.(8) should be applied for the prediction of shear strength of deep or short beams which can resist the increase of shear force after the occurrence of diagonal cracks. It is natural that eq.(8) should not be applied for the prediction of shear strength of slender beams which shall fail accompanied with the commencement of diagonal cracks. It may be considered that the limit of application of eq.(8) is represented by the point when shear force of the commencement of diagonal cracks is equivalent to shear strength predicted by eq.(8).

It is admitted that the equation which was proposed by Dr.Okamura and Dr.Higai can predict shear strength of slender beams without web reinforcement reasonably accurately[2]. It may be considered that the point where the value predicted by Okamura and Higai's equation is equal to the value predicted by eq.(8) is the limit of application of eq.(8).

5. CONCLUSION

(1). Parameters which influence shear strength of deep or short beams have been clarified by numerical research using non-linear FEM analysis. In this FEM analysis, cracks are modeled to so called "Smeared Crack". The effects of these parameters to the width and intensity of stress distribution of arch rib concrete can be estimated quantitatively. Finally equation for shear strength of deep or short beams without web reinforcement can be derived.

(2). Shear strength of deep or short beams should be influenced extremely by restrain conditions on supports and anchorage methods of main reinforcement. Therefore, in the refinement of experimental data, it should be noticed whether restrain on supports exists or not and anchorage of main reinforcement is complete or not.

(3). In the analysis of "Smeared Crack" as used in this report, it is difficult to simulate the final slip failure mode of beams along diagonal cracks. Therefore, it may be necessary to introduce appropriate failure criteria when diagonal failure mode of slender beams is simulated. For members such as deep beams dealt with in this report, however, this "Smeared Crack" analysis is available because crushing failure mode of web concrete is dominant. In consequence of this, numerical analysis may simulate behavior of beams just before final shear failure.

6. REFERENCES

[1]. Maekawa.K., Niwa.J. and Okamura.H.: "Computer Program 'COMM2' for Analyzing Reinforced Concrete", Proc. of JCI 2nd Colloquium on Shear Analysis of RC Structures, 1983.10

[2]. Okamura.H. and Higai.T.: "Proposed Design Equation for Shear Strength of Reinforced Concrete Beams Without Web Reinforcement", Proc. of JSCE., 1980.8